$$\times \left\{ \frac{a}{\pi} \times \left[\frac{(4NN_DR_C\eta_{RD}m_{RD})^{m_{RD}NN_D}\sqrt{m_{RD}NN_D}}{2\left(4NN_DR_C\eta_{RD}m_{SD}+P_S(\rho_{RD})^{2(\tau-1)}b\tilde{\delta}_{RD}^2\lambda^2\right)^{m_{SD}N}\sqrt{m_{RD}NN_D+1}}\ {}_2F_1\left(m_{RD}NN_D,\frac{1}{2};1+m_{RD}NN_D;\frac{1}{1+\frac{bP_S\tilde{\delta}_{RD}^2(\rho_{RD})^{2(\tau-1)}\lambda^2}{4NN_DR_C\eta_{RD}m_{RD}}}\right) \right] \right.$$
$$\left. -\frac{c}{2\sqrt{2\pi}}\left(\frac{b\tilde{\delta}_{RD}^2P_R(\rho_{RD})^{2(\tau-1)}\lambda^2}{2R_C\eta_{RD}m_{RD}NN_D}\right)^{m_{SD}N^2}\frac{\Gamma(m_{RD}NN_D+\frac{1}{2})}{\Gamma(m_{RD}NN_D+\frac{3}{2})}\times \mathsf{F}_A^{(1)}\left(m_{RD}NN_D+\frac{1}{2};\frac{1}{2},m_{RD}NN_D;m_{RD}NN_D+\frac{3}{2};\frac{1}{2};\frac{-m_{RD}NN_D}{\frac{b\tilde{\delta}_{RD}^2P_S(\rho_{RD})^{2(\tau-1)}\lambda^2}{2R_C\eta_{RD}}}\right) \right\} \quad (39)$$

$$P^E[\mathrm{X}_S[\tau]\to\mathrm{X}_i[\tau]]=\underbrace{P_E^{S\to D}\left[\mathrm{X}_S[\tau]\to\mathrm{X}_i[\tau]\right]}_{\substack{\textbf{Direct SD Transmission}\\\textbf{Error Probability}}}\times$$

$$\underbrace{P_E^{S\to R}}_{\substack{\textbf{Error Probability when relay}\\\textbf{decodes incorrectly}}}+\underbrace{(1-P_E^{S\to R})}_{\substack{\textbf{Probability when relay}\\\textbf{decodes correctly}}}\times \quad (40)$$

$$\underbrace{P_E^{SRD}\left(\mathrm{X}_S[\tau]\to\mathrm{X}_i[\tau]\right)}_{\substack{\textbf{SRD(Cooperation Mode Transmission)}\\\textbf{Transmission Error Probability}}}.$$

Substituting (20), (36) and (39) into (40) and employing the fact that $1-P_E^{S\to R}\approx1$ at high SNR in (40), yields the expression for the average end-to-end PEP

$P^E[\mathrm{X}_S[\tau]\to\mathrm{X}_i[\tau]]$ corresponds to the erroneous event $\mathrm{X}_S[\tau]\to\mathrm{X}_i[\tau]$ when $\mathrm{X}_S[\tau]$ confused for the $\mathrm{X}_i[\tau]$, as given in (41). Using the end-to-end error probability expression given in (41), the error bound for the ML decoding (optimum decoding) at the destination node corresponding to τ^{th} MIMO-STBC code-word block can now be readily obtained by considering the union bound over all the PEP terms corresponding to the $\mathrm{X}_S[\tau]\to\mathrm{X}_i[\tau]$ over-all the possible code-words $\mathbf{X}_S[\tau]\in\mathbf{C}.$ Finally, the per-block average PEP bound at the destination can be expressed, as given in (42).

$$P^E[\mathrm{X}_S[\tau]\to\mathrm{X}_i[\tau]]=$$

$$\left\{ \left\{ \frac{a}{\pi}\times \left[\frac{(4NN_DR_C\eta_{SD}m_{SD})^{m_{SD}NN_D}\sqrt{m_{SD}NN_D}}{2\left(4NN_DR_C\eta_{SD}m_{SD}+P_S(\rho_{SD})^{2(\tau-1)}b\tilde{\delta}_{SD}^2\lambda^2\right)^{m_{SD}N}\sqrt{m_{SD}NN_D+1}}\times \right.\right.\right.$$
$$\left.\left.\left. {}_2F_1\left(m_{SD}NN_D,\frac{1}{2};1+m_{SD}NN_D;\frac{1}{1+\frac{bP_S\tilde{\delta}_{SD}^2(\rho_{SD})^{2(\tau-1)}\lambda^2}{4NN_DR_C\eta_{SD}m_{SD}}}\right)\right] \right.\right. -$$
$$\left.\left. \left\{ \frac{c}{2\sqrt{2\pi}}\left(\frac{b\tilde{\delta}_{SD}^2P_S(\rho_{SD})^{2(\tau-1)}\lambda^2}{2R_C\eta_{SD}m_{SD}NN_D}\right)^{m_{SD}N^2}\frac{\Gamma(m_{SD}NN_D+\frac{1}{2})}{\Gamma(m_{SD}NN_D+\frac{3}{2})}\times \right.\right.\right.$$
$$\left.\left.\left. \mathsf{F}_A^{(1)}\left(m_{SD}NN_D+\frac{1}{2};\frac{1}{2},m_{SD}NN_D;m_{SD}NN_D+\frac{3}{2};\frac{1}{2};\frac{-m_{SD}NN_D}{\frac{b\tilde{\delta}_{SD}^2P_S(\rho_{SD})^{2(\tau-1)}\lambda^2}{2R_C\eta_{SD}}}\right)\right\} \right\}\right\}$$

$$\times$$

$$\left\{ \left\{ \frac{a}{\pi}\times \left[\frac{(4N^2R_C\eta_{SR}m_{SR})^{m_{SD}NN_D}\sqrt{m_{SD}NN_D}}{2\left(4NN_DR_C\eta_{SD}m_{SD}+P_S(\rho_{SD})^{2(\tau-1)}b\tilde{\delta}_{SD}^2\lambda^2\right)^{m_{SD}N}\sqrt{m_{SD}NN_D+1}}\times \right.\right.\right.$$
$$\left.\left.\left. {}_2F_1\left(m_{SD}NN_D,\frac{1}{2};1+m_{SD}NN_D;\frac{1}{1+\frac{bP_S\tilde{\delta}_{SD}^2(\rho_{SD})^{2(\tau-1)}\lambda^2}{4NN_DR_C\eta_{SD}m_{SD}}}\right)\right] \right.\right. -$$
$$\left.\left. \left\{ \frac{c}{2\sqrt{2\pi}}\left(\frac{b\tilde{\delta}_{SR}^2P_S(\rho_{SR})^{2(\tau-1)}\lambda^2}{2R_C\eta_{SR}m_{SR}N^2}\right)^{m_{SR}N^2}\frac{\Gamma(m_{SR}N^2+\frac{1}{2})}{\Gamma(m_{SR}N^2+\frac{3}{2})}\times \right.\right.\right.$$
$$\left.\left.\left. \mathsf{F}_A^{(1)}\left(m_{SR}N^2+\frac{1}{2};\frac{1}{2},m_{SR}N^2;m_{SR}N^2+\frac{3}{2};\frac{1}{2};\frac{-m_{SR}N^2}{\frac{b\tilde{\delta}_{SR}^2P_S(\rho_{SR})^{2(\tau-1)}\lambda^2}{2R_C\eta_{SR}}}\right)\right\} \right\}\right\}$$

$$+\left\{ \left\{ \frac{a}{\pi}\times \left[\frac{(4NN_DR_C\eta_{SD}m_{SD})^{m_{SD}NN_D}\sqrt{m_{SD}NN_D}}{2\left(4NN_DR_C\eta_{SD}m_{SD}+P_S(\rho_{SD})^{2(\tau-1)}b\tilde{\delta}_{SD}^2\lambda^2\right)^{m_{SD}N}\sqrt{m_{SD}NN_D+1}}\ {}_2F_1\left(m_{SD}NN_D,\frac{1}{2};1+m_{SD}NN_D;\frac{1}{1+\frac{bP_S\tilde{\delta}_{SD}^2(\rho_{SD})^{2(\tau-1)}\lambda^2}{4NN_DR_C\eta_{SD}m_{SD}}}\right)\right] \right\} - \right.$$
$$\left. \frac{c}{2\sqrt{2\pi}}\left(\frac{b\tilde{\delta}_{SD}^2P_S(\rho_{SD})^{2(\tau-1)}\lambda^2}{2R_C\eta_{SD}m_{SD}NN_D}\right)^{m_{SD}N^2}\frac{\Gamma(m_{SD}NN_D+\frac{1}{2})}{\Gamma(m_{SD}NN_D+\frac{3}{2})}\times \mathsf{F}_A^{(1)}\left(m_{SD}NN_D+\frac{1}{2};\frac{1}{2},m_{SD}NN_D;m_{SD}NN_D+\frac{3}{2};\frac{1}{2};\frac{-m_{SD}NN_D}{\frac{b\tilde{\delta}_{SD}^2P_S(\rho_{SD})^{2(\tau-1)}\lambda^2}{2R_C\eta_{SD}}}\right) \right\}$$

$$\times \left\{ \frac{a}{\pi} \times \left[\frac{(4NN_D R_C \eta_{RD} m_{RD})^{m_{RD}NN_D}\sqrt{m_{RD}NN_D}}{2\left(4NN_D R_C \eta_{RD} m_{SD} + P_S(\rho_{RD})^{2(\tau-1)}b\tilde{\delta}_{RD}^2\lambda^2\right)^{m_{SD}N}\sqrt{m_{RD}NN_D+1}}\; {}_2F_1\!\left(m_{RD}NN_D,\frac{1}{2};1+m_{RD}NN_D;\frac{1}{1+\frac{bP_S\tilde{\delta}_{RD}^2(\rho_{RD})^{2(\tau-1)}\lambda^2}{4NN_D R_C \eta_{RD} m_{RD}}}\right) \right] \right.$$
$$\left. -\frac{c}{2\sqrt{2\pi}}\left(\frac{b\tilde{\delta}_{RD}^2 P_R(\rho_{RD})^{2(\tau-1)}\lambda^2}{2R_C\eta_{RD}m_{RD}NN_D}\right)^{m_{SD}N^2}\frac{\Gamma(m_{RD}NN_D+\frac{1}{2})}{\Gamma(m_{RD}NN_D+\frac{3}{2})}\times \mathbf{F}_A^{(1)}\!\left(m_{RD}NN_D+\frac{1}{2};\frac{1}{2},m_{RD}NN_D;m_{RD}NN_D+\frac{3}{2};\frac{1}{2};\frac{-m_{RD}NN_D}{\frac{b\tilde{\delta}_{RD}^2 P_S(\rho_{RD})^{2(\tau-1)}\lambda^2}{2R_C\eta_{RD}}}\right)\right\}. \quad (41)$$

$$P^E \le \frac{1}{2\pi M_b}\times$$

$$\sum_{\tau=1}^{M_b}\sum_{i=1}^{|\mathbf{C}|}\left\{ \left[\frac{a}{\pi}\times\left[\frac{(4NN_D R_C \eta_{SD} m_{SD})^{m_{SD}NN_D}\sqrt{m_{SD}NN_D}}{2\left(4NN_D R_C \eta_{SD} m_{SD}+P_S(\rho_{SD})^{2(\tau-1)}b\tilde{\delta}_{SD}^2\lambda^2\right)^{m_{SD}N}\sqrt{m_{SD}NN_D+1}}\times {}_2F_1\!\left(m_{SD}NN_D,\frac{1}{2};1+m_{SD}NN_D;\frac{1}{1+\frac{bP_S\tilde{\delta}_{SD}^2(\rho_{SD})^{2(\tau-1)}\lambda^2}{4NN_D R_C \eta_{SD} m_{SD}}}\right)\right]\right.$$
$$\left.-\frac{c}{2\sqrt{2\pi}}\left(\frac{b\tilde{\delta}_{SD}^2 P_S(\rho_{SD})^{2(\tau-1)}\lambda^2}{2R_C\eta_{SD}m_{SD}NN_D}\right)^{m_{SD}N^2}\frac{\Gamma(m_{SD}NN_D+\frac{1}{2})}{\Gamma(m_{SD}NN_D+\frac{3}{2})}\times \mathbf{F}_A^{(1)}\!\left(m_{SD}NN_D+\frac{1}{2};\frac{1}{2},m_{SD}NN_D;m_{SD}NN_D+\frac{3}{2};\frac{1}{2};\frac{-m_{SD}NN_D}{\frac{b\tilde{\delta}_{SD}^2 P_S(\rho_{SD})^{2(\tau-1)}\lambda^2}{2R_C\eta_{SD}}}\right)\right]$$
$$\times\sum_{\substack{\mathbf{X}_S[\tau]\in\mathbf{C},\\ \mathbf{X}_S[\tau]\ne\mathbf{X}_l[\tau]}}\left[\frac{a}{\pi}\times\left[\frac{(4N^2 R_C \eta_{SR} m_{SR})^{m_{SD}NN_D}\sqrt{m_{SD}NN_D}}{2\left(4NN_D R_C \eta_{SD} m_{SD}+P_S(\rho_{SD})^{2(\tau-1)}b\tilde{\delta}_{SD}^2\lambda^2\right)^{m_{SD}N}\sqrt{m_{SD}NN_D+1}}\times {}_2F_1\!\left(m_{SD}NN_D,\frac{1}{2};1+m_{SD}NN_D;\frac{1}{1+\frac{bP_S\tilde{\delta}_{SD}^2(\rho_{SD})^{2(\tau-1)}\lambda^2}{4NN_D R_C \eta_{SD} m_{SD}}}\right)\right]\right.$$
$$\left.-\frac{c}{2\sqrt{2\pi}}\left(\frac{b\tilde{\delta}_{SR}^2 P_S(\rho_{SR})^{2(\tau-1)}\lambda^2}{2R_C\eta_{SR}m_{SR}N^2}\right)^{m_{SR}N^2}\frac{\Gamma(m_{SR}N^2+\frac{1}{2})}{\Gamma(m_{SR}N^2+\frac{3}{2})}\times \mathbf{F}_A^{(1)}\!\left(m_{SR}N^2+\frac{1}{2};\frac{1}{2},m_{SR}N^2;m_{SR}N^2+\frac{3}{2};\frac{1}{2};\frac{-m_{SR}N^2}{\frac{b\tilde{\delta}_{SR}^2 P_S(\rho_{SR})^{2(\tau-1)}\lambda^2}{2R_C\eta_{SR}}}\right)\right]$$
$$+\left[\frac{a}{\pi}\times\left[\frac{(4NN_D R_C \eta_{SD} m_{SD})^{m_{SD}NN_D}\sqrt{m_{SD}NN_D}}{2\left(4NN_D R_C \eta_{SD} m_{SD}+P_S(\rho_{SD})^{2(\tau-1)}b\tilde{\delta}_{SD}^2\lambda^2\right)^{m_{SD}N}\sqrt{m_{SD}NN_D+1}}\; {}_2F_1\!\left(m_{SD}NN_D,\frac{1}{2};1+m_{SD}NN_D;\frac{1}{1+\frac{bP_S\tilde{\delta}_{SD}^2(\rho_{SD})^{2(\tau-1)}\lambda^2}{4NN_D R_C \eta_{SD} m_{SD}}}\right)\right]-\right.$$
$$\left.\frac{c}{2\sqrt{2\pi}}\left(\frac{b\tilde{\delta}_{SD}^2 P_S(\rho_{SD})^{2(\tau-1)}\lambda^2}{2R_C\eta_{SD}m_{SD}NN_D}\right)^{m_{SD}N^2}\frac{\Gamma(m_{SD}NN_D+\frac{1}{2})}{\Gamma(m_{SD}NN_D+\frac{3}{2})}\times \mathbf{F}_A^{(1)}\!\left(m_{SD}NN_D+\frac{1}{2};\frac{1}{2},m_{SD}NN_D;m_{SD}NN_D+\frac{3}{2};\frac{1}{2};\frac{-m_{SD}NN_D}{\frac{b\tilde{\delta}_{SD}^2 P_S(\rho_{SD})^{2(\tau-1)}\lambda^2}{2R_C\eta_{SD}}}\right)\right]$$
$$\times\left[\frac{a}{\pi}\times\left[\frac{(4NN_D R_C \eta_{RD} m_{RD})^{m_{RD}NN_D}\sqrt{m_{RD}NN_D}}{2\left(4NN_D R_C \eta_{RD} m_{SD}+P_S(\rho_{RD})^{2(\tau-1)}b\tilde{\delta}_{RD}^2\lambda^2\right)^{m_{SD}N}\sqrt{m_{RD}NN_D+1}}\; {}_2F_1\!\left(m_{RD}NN_D,\frac{1}{2};1+m_{RD}NN_D;\frac{1}{1+\frac{bP_S\tilde{\delta}_{RD}^2(\rho_{RD})^{2(\tau-1)}\lambda^2}{4NN_D R_C \eta_{RD} m_{RD}}}\right)\right]\right.$$
$$\left.\left.-\frac{c}{2\sqrt{2\pi}}\left(\frac{b\tilde{\delta}_{RD}^2 P_R(\rho_{RD})^{2(\tau-1)}\lambda^2}{2R_C\eta_{RD}m_{RD}NN_D}\right)^{m_{SD}N^2}\frac{\Gamma(m_{RD}NN_D+\frac{1}{2})}{\Gamma(m_{RD}NN_D+\frac{3}{2})}\times \mathbf{F}_A^{(1)}\!\left(m_{RD}NN_D+\frac{1}{2};\frac{1}{2},m_{RD}NN_D;m_{RD}NN_D+\frac{3}{2};\frac{1}{2};\frac{-m_{RD}NN_D}{\frac{b\tilde{\delta}_{RD}^2 P_S(\rho_{RD})^{2(\tau-1)}\lambda^2}{2R_C\eta_{RD}}}\right)\right]\right\}. \quad (42)$$

3.2 Asymptotic error floor analysis

Now, in order to theoretically support our claims about the performance degradation due to imperfect-CSI and mobile nodes, it is useful to obtain the asymptotic error floors for the single relay S-DF protocol by ignoring N_0 in (10), (14) and (15) for single relay scenario, as expressed below [16-17],

$$\tilde{\eta}_{SD} = \rho_{SD}^{2(\tau-1)}\sigma_{\in SD}^2 + \left(1-\rho_{SD}^{2(\tau-1)}\right)\sigma_{eSD}^2, \quad (43)$$

$$\tilde{\eta}_{SR} = (\rho_{SR})^{2(\tau-1)}(\sigma_{\in SR})^2 + \left(1-(\rho_{SR})^{2(\tau-1)}\right)(\sigma_{eSR})^2, \quad (44)$$

$$\tilde{\eta}_{RD} = (\rho_{RD})^{2(\tau-1)}(\sigma_{\in RD})^2 + \left(1-(\rho_{RD})^{2(\tau-1)}\right)(\sigma_{eRD})^2, \quad (45)$$

Using $\tilde{\eta}_{SD}, \tilde{\eta}_{SR}$ and $\tilde{\eta}_{RD}$ in (42), one can readily obtain the asymptotic error floor for per block average PEP, as given in (46).

Various conditions arise due to nodes mobility:

When all nodes are static and perfect CSI condition

According to Jake's autocorrelation model [21], when all of the nodes are static, i.e., the relative speed between any two communicating nodes of them is zero, the correlation parameters ρ_{SR}, ρ_{SD} and ρ_{RD} reduce to 1. By considering this condition, the asymptotic limit for P^E is still given by (46), but with the following modified parameters: $\tilde{\eta}_{SD} = \sigma_{\in SD}^2, \tilde{\eta}_{SR} = \sigma_{\in SR}^2$, and $\tilde{\eta}_{RD} = \sigma_{\in RD}^2$. Furthermore, if the estimation processes throughout the network are perfect, i.e., $\sigma_{\in SD}^2 = \sigma_{\in SR}^2 = \sigma_{\in RD}^2 = 0$, the value of $\tilde{\eta}_{SD}, \tilde{\eta}_{SR}$ and $\tilde{\eta}_{RD}$ reduces to zero which reduces (46) to zero, i.e., the asymptotic error floor in (46), as expected, vanish, i.e., impact of node mobility is removed.

When source and destination nodes are static and relay node is mobile

Corollary 1: In DH single relay S-DF cooperative communication networks with perfect CSI, even though the relay is in motion, the system performance does not experience asymptotic limits if both source and destination are static.

Proof: In this scenario, $\rho_{SD} = 1$ while ρ_{SR} and ρ_{RD} are < 1. Under this condition, the asymptotic limit for P^E is still given by (46), but with the following modified parameters:

$$\tilde{\eta}_{SD} = \sigma_{\epsilon SD}^2, \ \tilde{\eta}_{SR} = (\rho_{SR})^{2(\tau-1)} \sigma_{\epsilon SR}^2 + \left(1 - (\rho_{SR})^{2(\tau-1)}\right)\sigma_{eSR}^2,$$

$$\tilde{\eta}_{RD} = (\rho_{RD})^{2(\tau-1)} \sigma_{\epsilon RD}^2 + \left(1 - (\rho_{RD})^{2(\tau-1)}\right)\sigma_{eRD}^2.$$

Furthermore, if the estimation processes throughout the network are perfect, i.e., $\sigma_{\epsilon SD}^2 = \sigma_{\epsilon SR}^2 = \sigma_{\epsilon RD}^2 = 0$, the value of $\tilde{\eta}_{SD}, \tilde{\eta}_{SR}$ and $\tilde{\eta}_{RD}$ reduces to zero which reduces (46) to zero, i.e., the asymptotic error floor in (46), as expected, vanish, i.e., impact of node mobility is removed. Despite that both scenarios (a) and (b) do not provide asymptotic limits in the case of perfect estimation, this does not mean that they provide same performance results over all the non-infinite SNR range. Later in the simulation results section, we will show that scenario (b) provides worse performance than scenario (a) due to the relay mobility.

When relay and source nodes are static and destination node is mobile

Corollary 2: In DH single relay S-DF cooperative communication networks, even though relay is static, the system performance is severely degraded by asymptotic limits if destination node is in motion.

Proof: When the destination node is in motion and the other nodes are static; $\rho_{SR} = 1$ while ρ_{SD} and ρ_{RD} are < 1. In this case,

the asymptotic limit is given in (46), but with the following modified parameters:

$$\tilde{\eta}_{SR} = \sigma_{\epsilon SR}^2, \tilde{\eta}_{SD} = \rho_{SD}^{2(\tau-1)} \sigma_{\epsilon SD}^2 + \left(1 - \rho_{SD}^{2(\tau-1)}\right)\sigma_{eSD}^2$$

and $\tilde{\eta}_{RD} = (\rho_{RD})^{2(\tau-1)} \sigma_{\epsilon RD}^2 + \left(1 - (\rho_{RD})^{2(\tau-1)}\right)\sigma_{eRD}^2.$

In this scenario, it is significant to note that the PEP term for the event when relay node decodes the MIMO STBC codeword correctly, i.e., $\underbrace{(1 - P_E^{S \to R})}_{\text{Probability when relay decodes correctly}}$ in (40) contributes to the asymptotic error floor for the per-block average PEP.

When relay and destination nodes are static and source node is mobile

Corollary 3: In DH single relay S-DF cooperative communication networks, even though relay is static, the system performance is severely degraded by asymptotic limits if the source node is in motion.

Proof: When the source node is in motion and the other nodes are static; $\rho_{RD} = 1$ while ρ_{SD} and ρ_{SR} are < 1. In this case, the asymptotic limit is given by (46), but with the following modified parameters:

$$\tilde{\eta}_{RD} = (\sigma_{\epsilon RD})^2, \ \tilde{\eta}_{SD} = \rho_{SD}^{2(\tau-1)} \sigma_{\epsilon SD}^2 + \left(1 - \rho_{SD}^{2(\tau-1)}\right)\sigma_{eSD}^2,$$

and $\tilde{\eta}_{SR} = (\rho_{SR})^{2(\tau-1)}(\sigma_{\epsilon SR})^2 + \left(1 - (\rho_{SR})^{2(\tau-1)}\right)(\sigma_{eSR})^2.$

In this scenario, it is significant to note that the PEP term for the event when relay node decodes the MIMO STBC codeword incorrectly, i.e., $\underbrace{P_E^{S \to R}}_{\text{Error Probability when relay decodes incorrectly}}$ in (40) contributes to the asymptotic error floor for the per-block average PEP.

$$P^F \leq$$

$$
\begin{aligned}
\frac{a}{\pi} \times \Bigg\{ & \Bigg\{ \frac{(4NN_a\tilde{\eta}_{SD}m_{SD}R_C)^{m_{SD}NN_D}\sqrt{m_{SD}NN_D}}{2\left(4NN_a\tilde{\eta}_{SD}m_{SD}R_C + (\rho_{SD})^{2(\tau-1)}b\tilde{\delta}_{SD}^2\lambda^2\right)^{m_{SD}N}\sqrt{m_{SD}NN_D+1}} \times \\
& {}_2F_1\left(m_{SD}NN_D, \frac{1}{2}; 1+m_{SD}NN_D; \frac{1}{1+\frac{b\tilde{\delta}_{SD}^2(\rho_{SD})^{2(\tau-1)}\lambda^2}{4NN_a\tilde{\eta}_{SD}m_{SD}R_C}}\right) \Bigg\} \\
& - \Bigg\{ \frac{c}{2\sqrt{2\pi}}\left(\frac{b\tilde{\delta}_{SD}^2(\rho_{SD})^{2(\tau-1)}\lambda^2}{2R_C\tilde{\eta}_{SD}m_{SD}NN_D}\right)^{m_{SD}N^2}\frac{\Gamma(m_{SD}NN_D+\frac{1}{2})}{\Gamma(m_{SD}NN_D+\frac{3}{2})} \times \\
& \mathbf{F}_A^{(1)}\left(m_{SD}NN_D+\frac{1}{2};\frac{1}{2}, m_{SD}NN_D; m_{SD}NN_D+\frac{3}{2};\frac{1}{2};\frac{-m_{SD}NN_D}{\frac{b\tilde{\delta}_{SD}^2(\rho_{SD})^{2(\tau-1)}\lambda^2}{2R_C\tilde{\eta}_{SD}}}\right) \Bigg\} \times
\end{aligned}
$$

$$
\sum_{\substack{\mathbf{X}_S[\tau]\in\mathbf{C}, \\ \mathbf{X}_S[\tau]\neq\mathbf{X}_I[\tau]}} \frac{a}{\pi} \times \Bigg\{ \Bigg\{ \frac{(4NN_aR_C\tilde{\eta}_{SR}m_{SR})^{m_{SR}N^2}\sqrt{m_{SR}N^2}}{2\left(4NN_aR_C\tilde{\eta}_{SR}m_{SR} + (\rho_{SR})^{2(\tau-1)}b\tilde{\delta}_{SR}^2\lambda^2\right)^{m_{SR}N^2}\sqrt{m_{SR}N^2+1}} \times {}_2F_1\left(m_{SR}N^2, \frac{1}{2}; 1+m_{SR}N^2; \frac{1}{1+\frac{b\tilde{\delta}_{SR}^2(\rho_{SR})^{2(\tau-1)}\lambda^2}{4N^2R_C\eta_{SR}m_{SR}}}\right) \Bigg\} - \Bigg\{ \frac{c}{2\sqrt{2\pi}}\left(\frac{b\tilde{\delta}_{SR}^2(\rho_{SR})^{2(\tau-1)}\lambda^2}{2R_C\tilde{\eta}_{SR}m_{SR}N^2}\right)^{m_{SR}N^2}\frac{\Gamma(m_{SR}N^2+\frac{1}{2})}{\Gamma(m_{SR}N^2+\frac{3}{2})} \times \mathbf{F}_A^{(1)}\left(m_{SR}N^2+\frac{1}{2};\frac{1}{2}, m_{SR}N^2; m_{SR}N^2+\frac{3}{2};\frac{1}{2};\frac{-m_{SR}N^2}{\frac{b\tilde{\delta}_{SR}^2P_S(\rho_{SR})^{2(\tau-1)}\lambda^2}{2R_C\tilde{\eta}_{SR}}}\right) \Bigg\} \Bigg\}
$$

$$
\sum_{\tau=1}^{M_b}\sum_{i=1}^{|\mathbf{C}|} \Bigg\{ \frac{a}{\pi} \times \Bigg\{ \frac{(4NN_a\tilde{\eta}_{SD}m_{SD}R_C)^{m_{SD}NN_D}\sqrt{m_{SD}NN_D}}{2\left(4NN_a\tilde{\eta}_{SD}m_{SD}R_C + (\rho_{SD})^{2(\tau-1)}b\tilde{\delta}_{SD}^2\lambda^2\right)^{m_{SD}N}\sqrt{m_{SD}NN_D+1}} \times {}_2F_1\left(m_{SD}NN_D, \frac{1}{2}; 1+m_{SD}NN_D; \frac{1}{1+\frac{b\tilde{\delta}_{SD}^2(\rho_{SD})^{2(\tau-1)}\lambda^2}{4NN_a\tilde{\eta}_{SD}m_{SD}R_C}}\right) \Bigg\}
$$

$$
+ \Bigg\{ \frac{c}{2\sqrt{2\pi}}\left(\frac{b\tilde{\delta}_{SD}^2(\rho_{SD})^{2(\tau-1)}\lambda^2}{2R_C\tilde{\eta}_{SD}m_{SD}NN_D}\right)^{m_{SD}N^2}\frac{\Gamma(m_{SD}NN_D+\frac{1}{2})}{\Gamma(m_{SD}NN_D+\frac{3}{2})} \times \mathbf{F}_A^{(1)}\left(m_{SD}NN_D+\frac{1}{2};\frac{1}{2}, m_{SD}NN_D; m_{SD}NN_D+\frac{3}{2};\frac{1}{2};\frac{-m_{SD}NN_D}{\frac{b\tilde{\delta}_{SD}^2(\rho_{SD})^{2(\tau-1)}\lambda^2}{2R_C\tilde{\eta}_{SD}}}\right) \Bigg\}
$$

$$
\times \Bigg\{ \frac{a}{\pi} \times \Bigg\{ \frac{(4NN_a\tilde{\eta}_{RD}m_{RD}R_C)^{m_{RD}NN_D}\sqrt{m_{RD}NN_D}}{2\left(4NN_a\tilde{\eta}_{RD}m_{RD}R_C + (\rho_{RD})^{2(\tau-1)}b\tilde{\delta}_{RD}^2\lambda^2\right)^{m_{RD}N}\sqrt{m_{RD}NN_D+1}} \times {}_2F_1\left(m_{RD}NN_D, \frac{1}{2}; 1+m_{RD}NN_D; \frac{1}{1+\frac{b\tilde{\delta}_{RD}^2(\rho_{RD})^{2(\tau-1)}\lambda^2}{4NN_a\tilde{\eta}_{RD}m_{RD}R_C}}\right) \Bigg\} -
$$

$$
\Bigg\{ \frac{c}{2\sqrt{2\pi}}\left(\frac{b\tilde{\delta}_{RD}^2(\rho_{RD})^{2(\tau-1)}\lambda^2}{2R_C\tilde{\eta}_{RD}m_{RD}NN_D}\right)^{m_{RD}N^2}\frac{\Gamma(m_{RD}NN_D+\frac{1}{2})}{\Gamma(m_{RD}NN_D+\frac{3}{2})} \times \mathbf{F}_A^{(1)}\left(m_{RD}NN_D+\frac{1}{2};\frac{1}{2}, m_{RD}NN_D; m_{RD}NN_D+\frac{3}{2};\frac{1}{2};\frac{-m_{RD}NN_D}{\frac{b\tilde{\delta}_{RD}^2(\rho_{RD})^{2(\tau-1)}\lambda^2}{2R_C\tilde{\eta}_{RD}}}\right) \Bigg\}.
$$

(46)

3.3 DO analysis and optimal power allocation

3.3.1 DO Analysis

In this sub-section we demonstrate the DO analysis and will develop a framework to evaluate the optimal source-relay power allocation factors, which will further enhance the end-to-end error performance of the relaying network. At high SNR, since the union bound is tight, the source and relay SNRs, $P_S / N_0, P_R / N_0 \to \infty$. We consider that each receiving terminal has perfect channel estimation, i.e., $\sigma_{\epsilon SD}^2 = \sigma_{\epsilon SR}^2 = \sigma_{\epsilon RD}^2 = 0$ and nodes are static, i.e., $\sigma_{eSD}^2 = \sigma_{eSR}^2 = \sigma_{eRD}^2 = 0$. Applying the above mentioned conditions in (41) and at high SNR, considering the

$$
\begin{aligned}
&P^E[\mathbf{X}_S[\tau] \to \mathbf{X}_i[\tau]] \\
&\approx \left[\begin{array}{l} \left(\dfrac{N_0}{P}\right)^{m_{SR}N^2 + m_{SD}NN_D} (K_1 - K_2)(K_1' - K_2') \times \dfrac{1}{\beta_0^{NN_D m_{SD} + N^2 m_{SR}}} + \\ \left(\dfrac{N_0}{P}\right)^{NN_D m_{SD}} \left(\dfrac{N_0}{P}\right)^{NN_D m_{RD}} (K_1' - K_2')(K_3' - K_4') \times \dfrac{1}{\beta_0^{NN_D m_{SD}} \beta_1^{NN_D m_{RD}}} \end{array} \right].
\end{aligned}
\tag{47}
$$

where, β_0 and β_1 are the optimal source-relay power factors,

$$\beta_0 = P_S / P, \ \beta_1 =$$

$$P_R / P, \ K_1 = \frac{a}{\pi} \left(\frac{2R_C m_{SR} N^2}{b\delta_{SR}^2} \right)^{m_{SR}N^2} \int_0^{\pi/2} (\sin^2 \theta)^{m_{SR}N^2} d\theta,$$

$$K_2 = \frac{c}{\pi} \left(\frac{2R_C m_{SR} N^2}{b\delta_{SR}^2} \right)^{m_{SR}N^2} \int_0^{\pi/4} (\sin^2 \theta)^{m_{SR}N^2},$$

$$K_1' = \frac{a}{\pi} \left(\frac{2R_C m_{SD} NN_D}{b\delta_{SD}^2} \right)^{m_{SD}NN_D} \int_0^{\pi/2} (\sin^2 \theta)^{m_{SD}NN_D} d\theta$$

$$K_2' = \frac{c}{\pi} \left(\frac{2R_C m_{SD} NN_D}{b\delta_{SD}^2} \right)^{m_{SD}NN_D} \int_0^{\pi/4} (\sin^2 \theta)^{m_{SD}NN_D} d\theta$$

$$K_3' = \frac{a}{\pi} \left(\frac{2R_C m_{RD} NN_D}{b\delta_{RD}^2} \right)^{m_{RD}NN_D} \int_0^{\pi/2} (\sin^2 \theta)^{m_{RD}NN_D} d\theta$$

$$K_4' = \frac{c}{\pi} \left(\frac{2R_C m_{RD} NN_D}{b\delta_{RD}^2} \right)^{m_{RD}NN_D} \int_0^{\pi/4} (\sin^2 \theta)^{m_{RD}NN_D} d\theta$$

Using the PEP expression expressed in (47) for the error event $X_S[\tau] \to X_i[\tau]$, the asymptotic PEP approximation of the above system can be obtained at high SNR employing the union bound, as given in (48). Asymptotically tight PEP expression expressed in (48) can be further simplified as,

$$P^E \le \Re_1 (N_0 / P)^{NN_D m_{SD} + N^2 m_{SR}} + \Re_2 (N_0 / P)^{NN_D m_{SD} + NN_D m_{RD}}, \tag{48}$$

where, the terms $\Re_1$ and $\Re_2$ are appropriately defined constant terms.

Depending upon the various values of the product of the DO and shape parameter of the fading links, various cases arise,

Case1: When the product of the DO and shape parameter of the RD fading link is greater than the product of the DO and shape parameter of the SR fading link, i.e., $NN_D m_{RD} > N^2 m_{SR}$. Then in high SNR regimes, the first term

dominating terms corresponding to $m, n = 0, 1$ in the identity $_2F_1(a, b; c; z) = \sum_{n=0}^{K} \frac{(a)_n (b)_n z^n}{(c)_n n!}$ for the Gauss Hypergeometric function and Appell hypergeometric function of two variables [22],

$$
\begin{aligned}
&F_A^{(1)}(\chi_1, \iota_1, \iota_1', \gamma''; x', y') = \\
&\sum_{m,n=0}^{\infty} \frac{(\chi_1)_{m+n} (\iota_1)_m (\iota_1')_n}{(\gamma'')_{m+n} \Gamma(m+1)\Gamma(n+1)} (x')^m (y')^n,
\end{aligned}
$$

where, $(x)_n$ is the Pochhammer symbols [22], one can simplify the expression in (41), as given in (47).

is the dominant term in PEP expression, PEP can be expressed as,

$$P^E \le \Re_1 (N_0 / P)^{NN_D m_{SD} + N^2 m_{SR}}.$$

So, DO can be derived as,

$$DO = - \lim_{P/N_0 \to \infty} \frac{\log(P^E)}{\log(P / N_0)} = NN_D m_{SD} + N^2 m_{SR}. \tag{49}$$

Case 2: When the product of the DO and shape parameter of the SR fading link is greater than the product of the DO and shape parameter of the RD fading link, i.e., $NN_D m_{RD} < N^2 m_{SR}$. Then in high SNR regimes, the second term is the dominant term in PEP expression, PEP can be written as,

$$P^E \le \Re_2 (N_0 / P)^{NN_D m_{SD} + NN_D m_{RD}}. \tag{50}$$

So, DO can be derived as,

$$DO = - \lim_{P/N_0 \to \infty} \frac{\log(P^E)}{\log(P / N_0)} = NN_D m_{SD} + NN_D m_{RD}. \tag{51}$$

Also, for the general case, when the product of the DO and shape parameter of the SR fading link is equal to the product of the DO and shape parameter of the RD fading link, i.e., $NN_D m_{RD} = N^2 m_{SR}$. Then in high SNR regimes, the DO can be expressed as,

$$
\begin{aligned}
DO &= \min(NN_D m_{SD} + N^2 m_{SR}, NN_D m_{SD} + NN_D m_{RD}) = \\
&NN_D m_{SD} + N \min(N m_{SR}, N_D m_{RD}).
\end{aligned}
\tag{52}
$$

3.3.2 Optimal power allocation

The expression (47) can be modeled as a CO problem for deriving the optimal source-relay power allocation factors β_0 and β_1.

CO problem is modeled as,

$$\min_{\beta_0, \beta_1} \left\{ \frac{\varpi_1}{\beta_0^{NN_D m_{SD} + N^2 m_{SR}}} + \frac{\varpi_2}{\beta_0^{NN_D m_{SD}} \beta_1^{NN_D m_{RD}}} \right\},$$
$$s.t. \ \beta_0 + \beta_1 \leq 1,$$

and,

$$\beta_0, \beta_1 \geq 0. \tag{53}$$

where, ϖ_1 and ϖ_2 are expressed below,

$$\varpi_1 = \left(\frac{N_0}{P} \right)^{m_{SR} N^2 + m_{SD} NN_D} (K_1 - K_2)(K_1' - K_2'),$$
$$\varpi_2 = \left(\frac{N_0}{P} \right)^{NN_D m_{SD} + NN_D m_{RD}} (K_1' - K_2')(K_3' - K_4'). \tag{54}$$

One can see that the KKT conditions-based CO framework can be employed for deriving the optimal source-relay power allocation factors β_0 and β_1. In the mathematical CO framework, the KKT conditions are 1st order necessary conditions for finding the optimal solution of nonlinear programming (NLP) [25], subject to the satisfaction of some regularity conditions. Allowing inequality constraints, the KKT will tend to NLP generalizes the concept of Lagrange multiplier which allows only equality constraints. Consider the following nonlinear minimization problem:

$$\min_{\beta_0, \beta_1} f(\beta_0, \beta_1) = \frac{\varpi_1}{\beta_0^{NN_D m_{SD} + N^2 m_{SR}}} + \frac{\varpi_2}{\beta_0^{NN_D m_{SD}} \beta_1^{NN_D m_{RD}}},$$
$$s.t. \ \beta_i \geq 0, \quad i = 0,1. \tag{55}$$

where, ϖ_1 and ϖ_2 are given as,

$$\varpi_1 = \left(\frac{N_0}{P} \right)^{m_{SR} N^2 + m_{SD} NN_D} (K_1 - K_2)(K_1' - K_2'), \tag{56}$$

$$\varpi_2 = \left(\frac{N_0}{P} \right)^{NN_D m_{SD}} \left(\frac{N_0}{P} \right)^{NN_D m_{RD}} (K_1' - K_2')(K_3' - K_4'). \tag{57}$$

By changing $\beta_i \geq 0$ to $-\beta_i \leq 0$ and noting that the above CO problem is minimization problem, the Lagrangian based mathematical framework is given as,

$$L'(\beta_0, \beta_1) =$$
$$\frac{\varpi_1}{\beta_0^{NN_D m_{SD} + N^2 m_{SR}}} + \frac{\varpi_2}{\beta_0^{NN_D m_{SD}} \beta_1^{NN_D m_{RD}}} + \zeta'(\beta_0 + \beta_1 - 1), \ \zeta' > 0 \tag{58}$$

where, ζ' denotes the Lagrange multiplier. Differentiating $L'(\beta_0, \beta_1)$ with respect to β_0, we get,

$$\frac{\partial L'(\beta_0, \beta_1)}{\partial \beta_0} = \frac{-\varpi_1 (NN_D m_{SD} + N^2 m_{SR})}{\beta_0^{NN_D m_{SD} + N^2 m_{SR}}}$$
$$+ \frac{-\varpi_2 (NN_D m_{SD})}{\beta_0^{NN_D m_{SD} + 1} \beta_1^{NN_D m_{RD}}} + \zeta', \tag{59}$$

Putting (59) equal to zero, we get,

$$\zeta' = \frac{\varpi_1 (NN_D m_{SD} + N^2 m_{SR})}{\beta_0^{NN_D m_{SD} + N^2 m_{SR}}} + \frac{\varpi_2 (NN_D m_{SD})}{\beta_0^{NN_D m_{SD} + 1} \beta_1^{NN_D m_{RD}}}, \tag{60}$$

Differentiating $L'(\beta_0, \beta_1)$ with respect to β_1 and putting the resultant expression equal to zero, we get,

$$\zeta' = \frac{\varpi_2 (NN_D m_{RD})}{\beta_0^{NN_D m_{SD}} \beta_1^{NN_D m_{RD} + 1}}, \tag{61}$$

Substituting the value of ζ' obtained in (61) into (60), we get,

$$(1 - \beta_0)^{NN_D m_{RD} + 1} \varepsilon - (\beta_0)^{N^2 m_{SR} + 1} + (1 - \beta_0)(\beta_0)^{N^2 m_{SR}} = 0. \tag{62}$$

where, ε is expressed in (63). Further, we can find out the solution of the quadratic expression given in the equation (62) by using standard mathematical computing software such as MATHEMATICA or MATLAB.

$$\varepsilon = \begin{cases} \dfrac{(NN_D m_{SD} + N^2 m_{SR})(K_1 - K_2)}{(NN_D m_{SD})(K_3' - K_4')} \left(\dfrac{N_0}{P} \right)^{N^2 m_{SR} - NN_D m_{RD}} & ; \ N^2 m_{SR} > NN_D m_{RD} \\ \dfrac{(NN_D m_{SD} + N^2 m_{SR})(K_1 - K_2)}{(NN_D m_{SD})(K_3' - K_4')} \left(\dfrac{N_0}{P} \right)^{NN_D m_{RD} - N^2 m_{SR}} & ; \ N^2 m_{SR} < NN_D m_{RD} \end{cases} \tag{63}$$

4. SIMULATION RESULTS

Monte Carlo (MC) simulations are conducted to confirm the accuracy of the theoretical results for the considered MIMO STBC based S-DF cooperative communication protocol over time selective Nakagami-m fading channel conditions considering imperfect CSI and node mobility conditions. Due to nodes mobility, the system's links are characterized by time-selective fading channels, which are modeled by the AR1 process, and due to incorrect CSI estimation, the estimated channel variances are assumed to be corrupted by Gaussian errors. For such a system model, an approach is proposed to derive a tight approximate expression for the system's conditional PEP. This approach is based on utilizing the AR1 model to derive exact expressions for the per block average PEP of the Alamouti decoder's decision variables, and on benefiting from the central limit theorem to approximate some of the non-Gaussian interference and noise terms. The

obtained conditional PEP expression is function of both the fading channel correlation parameters and the estimation error variances, and thus, it is valid for mobile as well as static nodes for imperfect as well as perfect channel state information estimation processes. We consider S-DF relaying protocol and assume that the relay can check whether the decoding result is correct or not. Per block average PEP performance is investigated for both equal and optimal power allocation scenarios. To investigate the accuracy of the investigation for M-PSK signals, we employ M = 4 to check the M-PSK results. Figure 2. shows the PEP performance of dual phase DH relaying protocol over time selective Nakagami-m channel with imperfect CSI and node mobility for equal and optimal

power allocation. The results show that analytical results are in exact match with the simulated results at high SNR regimes and the per block average PEP performance for optimal power is better than PEP performance for equal power allocation. Figure 3. shows the per block average PEP performance of MIMO Alamouti STBC S-DF relaying protocol with QPSK modulation for various node mobility scenarios. Results show that for the network conditions when, $\rho_{SR} < 1, \rho_{RD} = 1, \rho_{SD} < 1$, source mobility significantly degrades the per block average PEP performance in contrast to the network condition with only relay is mobile, i.e., $\rho_{SR} < 1, \rho_{RD} < 1, \rho_{SD} = 1$.
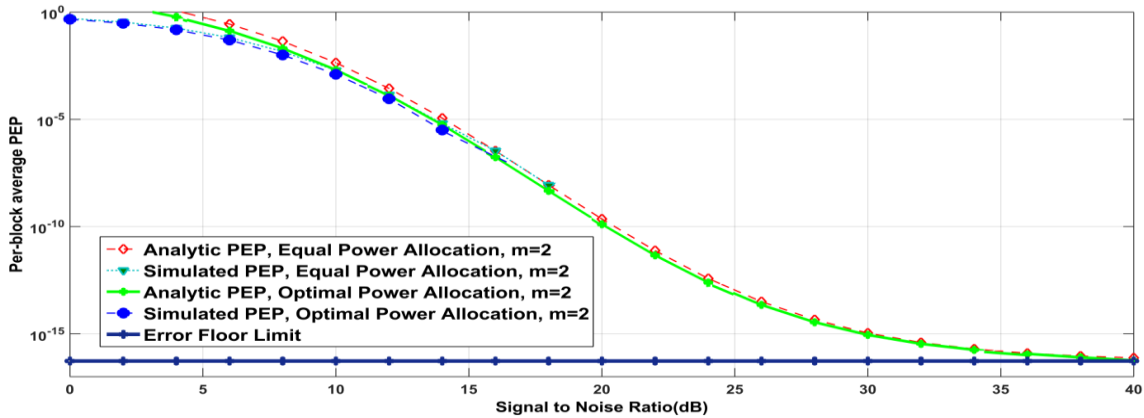
Figure 2. Per block average PEP vs. SNR in dB of MIMO Alamouti STBC S-DF relaying protocol with QPSK modulation for optimal and equal power allocation with $f_C = 5.9GHz, R_S = 9.6\,kbps, N_0 = 1, R_C = 1, N = N_D = 2, \sigma_{\epsilon_i}^2 = 0.01,$

$\sigma_{e_i}^2 = 0.01; i \in \{SD, SR, RD\}, v_p = 50mph, \delta_{SD}^2 = 2, \delta_{SR}^2 = 2, \delta_{RD}^2 = 2$ and optimal power allocation factors are $\beta_0 = 0.3843,$

$\beta_1 = 0.3078$ and $\beta_2 = 0.3078, M_b = 5,$ respectively
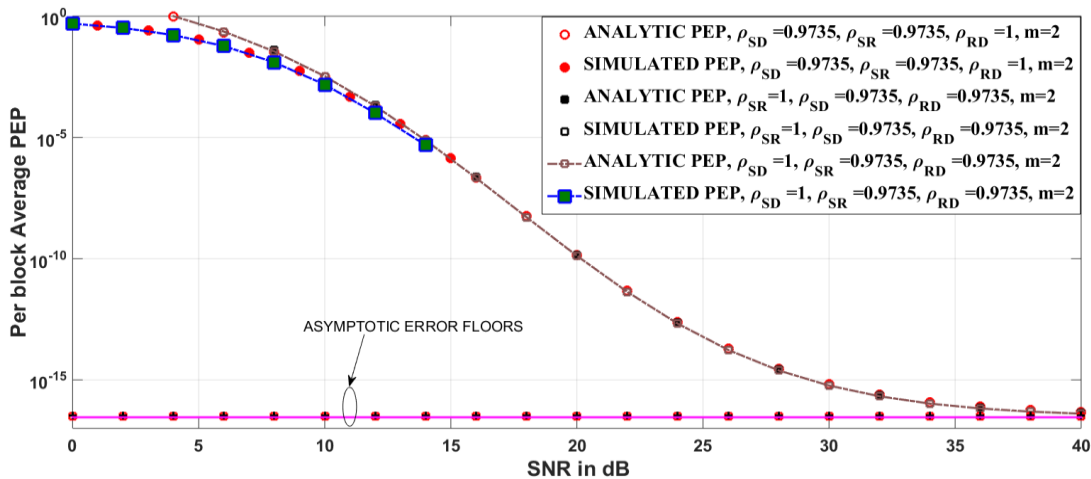
Figure 3. Per block average PEP vs. SNR in dB of MIMO Alamouti STBC S-DF relaying protocol with QPSK modulation for various node mobility scenarios. Simulation parameters are: $\beta_0 = 0.333, \beta_1 = 0.333, \beta_2 = 0.333 f_C = 5.9GhZ, R_S = 12Kbps,$

$N_0 = 1, R_C = 1, N = N_D = 2, \sigma_{\epsilon_i}^2 = 0.001, \sigma_{e_i}^2 = 0.01; i \in \{SD, SR, RD\}, M_b = 5, v_p = 55mph, \delta_{SD}^2 = 2, \delta_{SR}^2 = 2, \delta_{RD}^2 = 2$

5. CONCLUSION

This paper comprehensively investigates the performance of DH MIMO-STBC cooperative wireless systems over time-selective and possibly i.n.i.d. Nakagami-m fading links. CF expressions have been derived for the per-block average PEP with time selectivity arises due to node mobility and imperfect

CSI. The results show that analytical results are in exact match with the simulated results at high SNR regimes and the per block average PEP performance for optimal power is better than PEP performance for equal power allocation. Specifically, we found that the source mobility significantly degrades the per block average PEP performance in contrast to the network condition with only relay and destination nodes are mobile.

For other node mobility scenarios, the system is constrained by an asymptotic error floor with a higher SNR regime. Results show that with increase in the fading severity parameter per-block average PEP performance improves.

REFERENCES

[1] Li, S.C., Xu, L.D., Zhao, S.S (2018). 5G internet of things: A survey. Journal of Industrial Information Integration, 10: 1-9. https://doi.org/10.1016/j.jii.2018.01.005

[2] Mohamed, E., Abdelaziz, A., Salama, A.S., Riad, A.M., Muhammad, K., Sangaiah, A.K. (2018). A hybrid model of internet of things and cloud computing to manage big data in health services applications. Future Generation Computer Systems, 86: 1383-1394. https://doi.org/10.1016/j.future.2018.03.005

[3] Mehdi, S., Muhaidat, S., Liang, J. (2012). Amplify-and-forward selection cooperation over Rayleigh fading channels with imperfect CSI. IEEE Transactions on Wireless Communications, 11(1): 199-209. https://doi.org/10.1109/TWC.2011.120611.11006

[4] Lee, S., Su, W.F., Batalama, S., Matyjas, J.D. (2010). Cooperative decode-and-forward ARQ relaying: Performance analysis and power optimization. IEEE Transactions on Wireless Communications, 9(8): 2632-2642. https://doi.org/10.1109/TWC.2010.062310.091554

[5] Dong, Y., Hossain, M.J., Cheng, J. (2016). Performance of wireless powered amplify and forward relaying over nakagami- fading channels with nonlinear energy harvester. IEEE Communications Letters, 20(4): 672-675. https://doi.org/10.1109/lcomm.2016.2528260

[6] Van Nguyen, B., Kim, K. (2016). Performance analysis of amplify-and-forward systems with single relay selection in correlated environments. Sensors (Basel, Switzerland), 16(9): 1472-1486. https://doi.org/10.3390/s16091472

[7] Bhatnagar, M.R., Hjorungnes, A. (2011). ML decoder for decode-and-forward based cooperative communication system. IEEE Transactions on Wireless Communications, 10(12): 4080-4090. https://doi.org/10.1109/TWC.2011.100611.101341

[8] Soni, S., Rawal, D., Sharma, N., Jayakody, D.N.K. (2018). Selective DF based multiple relayed cooperative system with M-QAM signaling. 2018 IEEE 29th Annual International Symposium on Personal, Indoor and Mobile Radio Communications (PIMRC), pp. 147-152. https://doi.org/10.1109/PIMRC.2018.8580894

[9] Varshney, N., Krishna, A.V., Jagannatham, A.K. (2015). Selective DF protocol for MIMO STBC based single/multiple relay cooperative communication: End-to-end performance and optimal power allocation. IEEE Transactions on Communications, 63(7): 2458-2474. https://doi.org/10.1109/TCOMM.2015.2436912

[10] Vikash, S., Kumar, I., Shankar, R., Mishra, R.K. (2018). Analysis of transmit antenna selection based selective decode forward cooperative communication protocol. Traitement du Signal, 35(1): 47-60. https://doi.org/10.3166/ts.35.47-60

[11] Shankar, R., Kumar, I., Mishra, R.K. (2019). Outage probability analysis of MIMO-OSTBC relaying network over Nakagami-m fading channel conditions, Traitement du Signal, 36(1): 59-64. https://doi.org/10.18280/ts.360108

[12] Shankar, R., Pandey, K.N., Kumari, A., Sachan, V., Mishra, R.K. (2017). C(0) protocol based cooperative wireless communication over Nakagami-m fading channels: PEP and SER analysis at optimal power. 2017 IEEE 7th Annual Computing and Communication Workshop and Conference (CCWC), Las Vegas, NV, 1-7. https://doi.org/10.1109/CCWC.2017.7868399

[13] Ravi, S., Mishra, R.K. (2018). An investigation of S-DF cooperative communication protocol over keyhole fading channel. Physical Communication, 29: 120-140. https://doi.org/10.1016/j.phycom.2018.04.027

[14] Yazid, K., Matalgah, M.M. (2015). Conventional and best-relay-selection cooperative protocols under nodes-mobility and imperfect-CSI impacts: BER performance. 2015 IEEE Wireless Communications and Networking Conference (WCNC), pp. 105-110. https://doi.org/10.1109/WCNC.2015.7127453

[15] Chao, L., Xu, Y., Xia, J.J., Zhao, J.H. (2018). Protecting secure communication under UAV smart attack with imperfect channel estimation. IEEE Access, 6: 76395-76401. https://doi.org/10.1109/ACCESS.2018.2880979

[16] Varshney, N., Jagannatham, A.K., Varshney, P.K. (2018). Cognitive MIMO-RF/FSO cooperative relay communication with mobile nodes and imperfect channel state information. IEEE Transactions on Cognitive Communications and Networking, 4(3): 544-555. https://doi.org/10.1109/TCCN.2018.2844827

[17] Agarwal, A., Varshney, N., Jagannatham, A.K. (2016). Performance analysis of multi-relay selective DF based OFDM cooperative systems over time selective links with imperfect CSI. 2016 IEEE Region 10 Conference (TENCON), Singapore, pp. 3220-3223. https://doi.org/10.1109/TENCON.2016.7848644

[18] Ge, X., Cheng, H., Mao, G., Yang, Y., Tu, S. (2016). Vehicular communications for 5G cooperative small-cell networks. IEEE Transactions on Vehicular Technology, 65(10): 7882-7894. https://doi.org/10.1109/TVT.2016.2539285

[19] Raymond, J.W., Olwal, T.O., Kurien, A.M. (2018). Cooperative communications in machine to machine (M2M): solutions, challenges and future work. IEEE Access, 6: 9750-9766. https://doi.org/10.1109/ACCESS.2018.2807583

[20] Baddour, K.E., Beaulieu, N.C. (2005). Autoregressive modeling for fading channel simulation. IEEE Transactions on Wireless Communications, 4(4): 1650-1662. https://doi.org/10.1109/TWC.2005.850327

[21] Boyd, S., Kim, S.J., Vandenberghe, L., Hassibi, A. (2007). A tutorial on geometric programming. Optimization and Engineering, 8(1): 67-127. https://doi.org/10.1007/s11081-007-9001-7

[22] Jeffrey, A., Zwillinger, D. (2007). Table of integrals, series, and products. Elsevier.

[23] Zhou, Y., Cheng, N., Lu, N., Shen, X.S. (2015). Multi-UAV-aided networks: Aerial-ground cooperative vehicular networking architecture. IEEE Vehicular Technology Magazine, 10(4): 36-44. https://doi.org/10.1109/MVT.2015.2481560

[24] Kumbhani, B., Kshetrimayum, R.S. (2017). MIMO wireless communications over generalized fading channels. CRC Press.

[25] Raymond, J.W., Olwal, T.O., Kurien, A.M. (2018). Cooperative communications in machine to machine (M2M): Solutions, challenges and future work. IEEE Access, 6: 9750-9766. https://doi.org/10.1109/ACCESS.2018.2807583

[26] Du, Z., Cheng, J.L., Beaulieu, N.C. (2006). Accurate error-rate performance analysis of OFDM on frequency-selective Nakagami-m fading channels. IEEE Transactions on Communications, 54(2): 319-328. https://doi.org/10.1109/TCOMM.2005.863729